

Al₂O₃ coating with a Ni-based buffer layer: Preparation, characterization and electrical insulating properties

Lingnan Wu, Lixin Song^{*}, Jiehua Wu, Lili Zhao, Chunjun Jiang

Shanghai Institute of Ceramics, Chinese Academy of Sciences, 1295 Dingxi Road, Shanghai 200050, PR China

Received 5 October 2005; received in revised form 11 November 2005; accepted 6 December 2005

Available online 11 May 2006

Abstract

Al₂O₃ coatings, with a Ni-based buffer layer (Ni or NiAl), were deposited on a Cu substrate by electron beam evaporation (EBE). The Al₂O₃ coatings were amorphous of good stoichiometry and their surface was undulated and continuous. The Ni-based buffer layer played a key role on improving the adhesion of the Al₂O₃ coatings to the substrate. The diffusion of Cu from the substrate into the Al₂O₃ coating at high temperature was suppressed by the buffer layer. Excellent resistivity ($10^{15} \Omega \text{ cm}$) and high breakdown voltage (110 kV/mm) have been obtained.

© 2006 Published by Elsevier Ltd and Techna Group S.r.l.

Keywords: Al₂O₃ coating; Electron beam evaporation; Electrical insulating properties

1. Introduction

Recently, much attention has been paid on electrical insulating coatings used at high temperature for their potential application in special electromotors. The coatings are required to be used at temperature up to 600 °C, where organic insulating materials are unsuitable. Al₂O₃ is a promising coating material due to its high electrical resistivity, and good chemical and thermal stabilities. Many studies have demonstrated that Al₂O₃ is applicable in DRAMs [1], gate insulators [2], film capacitors [3] and so on. It is reasonable to believe that Al₂O₃ could be utilized in preparing good insulating coating for use at high temperature.

Al₂O₃ coatings have been prepared by various methods including sol–gel [4,5], chemical vapor deposition (CVD) [6,7] and physical vapor deposition (PVD) [8–11]. Organic precursors are usually used in sol–gel and CVD techniques. Nevertheless, coatings prepared by these methods mostly have porous structure, which will cause a drop of the breakdown voltage. PVD (sputtering or evaporation) is widely utilized to prepare Al₂O₃ coatings especially in the microelectronics industry. At present, Al₂O₃ coatings for electrical insulating application are mainly deposited by sputtering, while studies on Al₂O₃ coating prepared by electron beam evaporation (EBE)

are seldom reported [12,13]. At constant temperature small amount of moisture or impurities would degrade insulating properties dramatically. Indeed EBE technique operated in a high vacuum environment can ensure the achievement of a dense and pure coating, which is favorable for electrical insulating properties.

In this paper, we prepared a dense and pure Al₂O₃ coating on a Cu substrate by the EBE technique. A Ni-based alloy was introduced as a buffer layer to alleviate the mismatch of thermal expansion coefficient between the Cu substrate ($10^{-5}/^{\circ}\text{C}$) and the Al₂O₃ coating ($10^{-6}/^{\circ}\text{C}$), and to suppress the diffusion of Cu into the Al₂O₃ coating. An Al₂O₃ coating without buffer layer was also prepared for comparison. The electrical resistivity, breakdown voltage, and microstructure of Ni or NiAl/Al₂O₃ coating were studied.

2. Experimental

At first, the Cu substrates (20 mm × 200 mm) were cleaned by immersing in a mixture of nitric acid, phosphoric acid and acetic acid for 5 min. Afterwards, a Ni-based buffer layer, was deposited on the surface of the Cu substrate by thermal resistance either from Ni (99.99% purity) or from NiAl (99.99% purity, weight ratio of Ni:Al = 95:5) source. The base pressure of the deposition chamber was below $5 \times 10^{-3} \text{ Pa}$. Subsequently, using Al₂O₃ pellets (99.99% purity) with diameter of 1–2.5 mm as EBE source, the Al₂O₃ coating

^{*} Corresponding author.

E-mail address: lxsong@sunm.shcnc.ac.cn (L. Song).

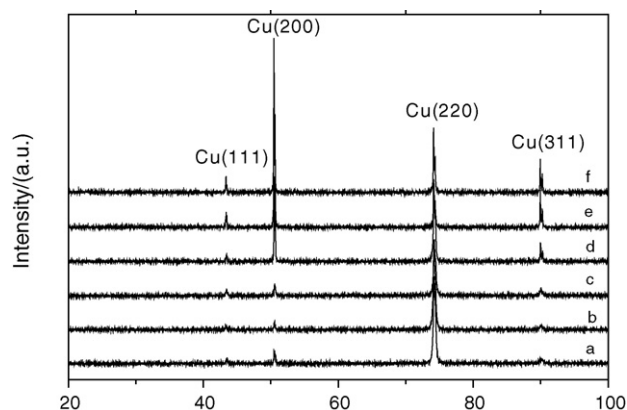


Fig. 1. XRD patterns of (a) Al_2O_3 coating; (b) Al_2O_3 coating after thermal cycling; (c) Ni/ Al_2O_3 coating; (d) Ni/ Al_2O_3 coating after thermal cycling; (e) NiAl/ Al_2O_3 coating; (f) NiAl/ Al_2O_3 coating after thermal cycling.

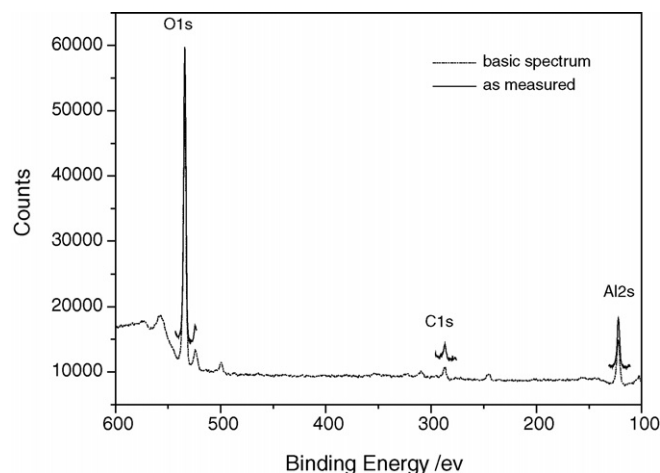


Fig. 2. XPS spectrum of Ni/ Al_2O_3 coating.

was deposited on the surface of the buffer layer with an electron beam power varying from 1.6 to 2.0 kW and substrate temperature of 250 °C. The deposition rate was controlled about at 100–150 nm/min.

Thermal cycling tests were conducted by rapidly heating the deposited Al_2O_3 coatings from room temperature to 600 °C, keeping them at this temperature for 5 min, then quenching them down to room temperature in air. Electrical resistivity and breakdown voltage were measured by a high resistance meter (HP4312A) and a direct current transistor manostat. The surface and cross section morphologies were observed by AFM (SPI3800 Atomic Force Microscope) and SEM (JSM-6700F Field Emission Scanning Electron Microscope). The structural characteristics were determined by XRD (Rigaku B/Max-2550V). The chemical composition and depth profiles were analyzed by Microlab310F Auger Microprobe. The thickness of the coatings was measured by a profilometer (Taylor–Hobson Talystep Surface Profilometer).

3. Results and discussion

3.1. XRD patterns

X-ray patterns of Al_2O_3 coatings with and without Ni-based buffer layer are shown in Fig. 1. It can be observed from Fig. 1 that all the peaks come from the Cu substrate. No Al_2O_3

diffraction peaks have been detected, indicating of the amorphous structure of the deposited Al_2O_3 coatings. No crystallization has been observed for the Al_2O_3 coatings even after thermal cycling at 600 °C.

3.2. XPS analysis

The X-ray photoelectron spectroscopy (XPS) of the Ni/ Al_2O_3 coating is shown in Fig. 2. The energy position of the Al 2s corresponds to that of Al_2O_3 . Through the analysis of XPS spectrum, it can be concluded that the Ni/ Al_2O_3 coating has a good stoichiometry and that the coating process does not affect negatively the electrical insulating properties since there is no oxygen deficiency, probably because the atomic kinetic energy of the evaporated Al_2O_3 particles was not sufficient to break Al–O bond in the EBE process. Furthermore, the coating does not contain impurities from Ni or Cu that would degrade the electrical insulating properties of the Al_2O_3 coating.

3.3. AFM investigation of the surface morphology

The AFM morphology of the Ni/ Al_2O_3 coating before and after thermal cycling is shown in Fig. 3. Undulating and continuous surfaces can be observed, which may be attributed to the unpolished Cu substrate. From Fig. 3(a) and (b), no evident changes have been observed for the Ni/ Al_2O_3 coating

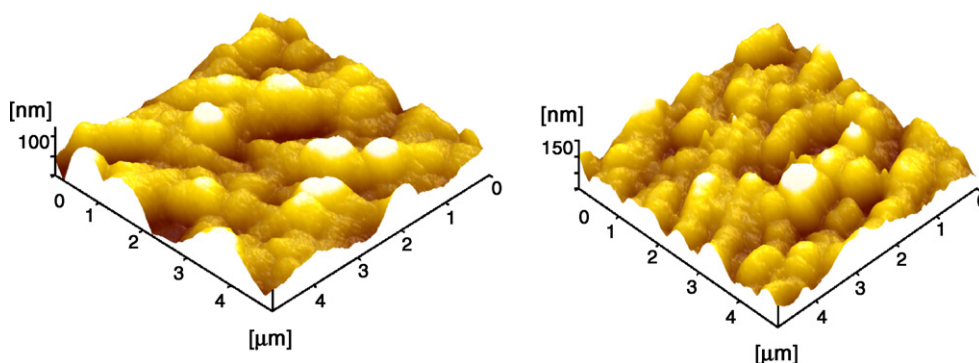


Fig. 3. AFM morphology of NiAl/ Al_2O_3 coating (a) before and (b) after thermal cycling.

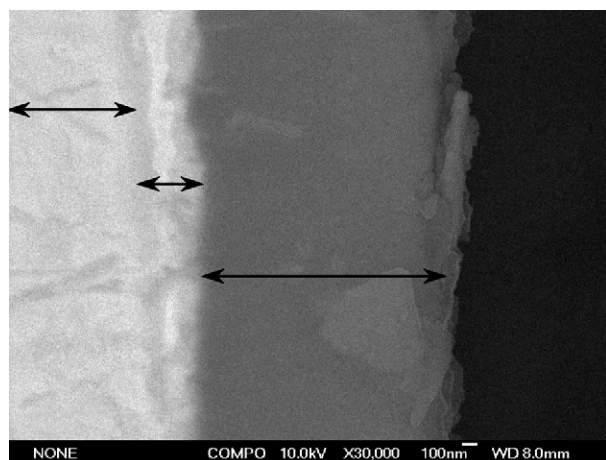


Fig. 4. SEM morphology of polished cross section of NiAl/Al₂O₃ coating after thermal cycling.

before and after thermal cycling. The surface morphology does not show evidence of pores, which is beneficial to the electrical insulating properties.

3.4. SEM cross section morphology

The SEM morphology of a polished cross section of the NiAl/Al₂O₃ coating after thermal cycling is shown in Fig. 4. The Cu substrate, NiAl buffer layer and the Al₂O₃ coating are well evidenced by their different contrast. The thickness of the Al₂O₃ coating is about 1 μ m (in Fig. 4) in agreement with the result of profilometer measurement. The interface of the NiAl buffer layer and Cu substrate is blurred due to their close atomic number, while that of NiAl buffer layer and Al₂O₃ coating is clearly distinguished. Furthermore, it also can be seen that a dense, crack-free and well-adhered Al₂O₃ coating with no trace of column structure is obtained. Thus, we can conclude that the Ni-based buffer layer played a key role on improving the adhesion of the Al₂O₃ coating to the substrate, probably because of the closely matched crystal structure and crystal constant between Cu and Ni, and of the strong

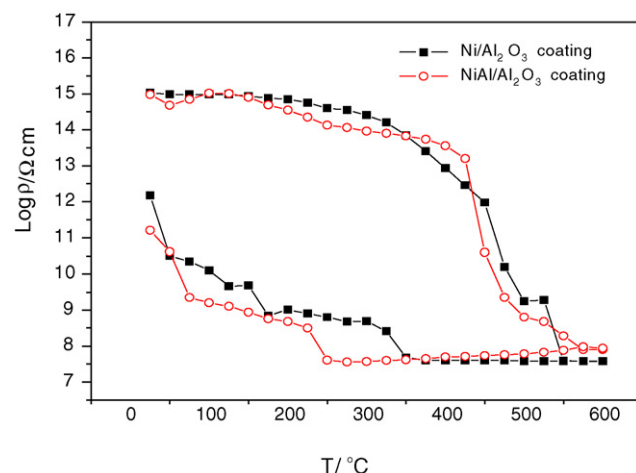


Fig. 6. Dependence of resistivity on temperature for Ni/Al₂O₃ coating and NiAl/Al₂O₃ coating.

interface (adhesion work up to 380 MJ/m²) between Ni and Al₂O₃ [14].

3.5. AES depth profiles

AES depth profiles were used to determine the diffusion behaviour of the interface at high temperature. AES depth profiles of Al₂O₃ coating without and with NiAl buffer layer after thermal cycling are given in Fig. 5. The etching end point was about 20 nm away from the interface of the substrate and the Al₂O₃ coating (Fig. 5(a)) or the interface of the buffer layer and the Al₂O₃ coating (Fig. 5(b)). In Fig. 5(a), peaks around 919 and 836 eV correspond to O and Al of Al₂O₃, indicating that the Cu diffused from the substrate into the Al₂O₃ coating when heated to 600 °C. However, in Fig. 5(b), all peaks correspond to O and Al of Al₂O₃, and no peaks from Ni or Cu have been detected. This suggested that the diffusion of Cu from the substrate into the Al₂O₃ coating at high temperature was effectively suppressed by the buffer layer, and that the buffer layer did not diffuse into the Al₂O₃ coating.

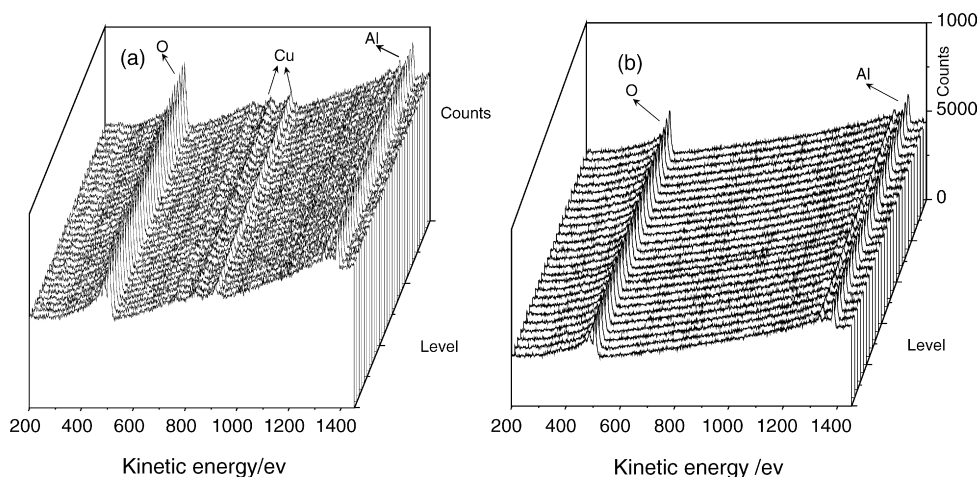


Fig. 5. Auger electron depth profiles of (a) single Al₂O₃ coating and (b) NiAl/Al₂O₃ coating after thermal cycling.

Table 1
Comparison of breakdown voltage of Al_2O_3 coatings before and after thermal cycling

Samples	Breakdown voltage (kV/mm)	
	Before thermal cycling	After thermal cycling
Al_2O_3 coating	100	50
$\text{Ni}/\text{Al}_2\text{O}_3$ coating	100	60–80
$\text{NiAl}/\text{Al}_2\text{O}_3$ coating	110	80

3.6. Electrical insulating properties

The dependence of coating resistivity on temperature up to 600 °C for the $\text{Ni}/\text{Al}_2\text{O}_3$ and $\text{NiAl}/\text{Al}_2\text{O}_3$ coating is illustrated in Fig. 6. A behaviour similar to the hysteresis loop is observed. With temperature increasing from 25 °C to 600 °C resistivity decreased from 10^{15} to 10^{7-8} Ω cm, and then increased to 10^{12} Ω cm with the decrease of temperature from 600 to 25 °C. Nevertheless, the coatings resistivity does not reach the original value after thermal cycling. Further experiments revealed that the same trend could still be observed after thermal cycling for seven times. Nevertheless, after eight cycling tests the coating was experienced to lose its electrical insulating function.

The breakdown voltages of Al_2O_3 coatings before and after thermal cycling are shown in Table 1. The results show that the deposited Al_2O_3 coating with and without Ni-based buffer layer both exhibit high breakdown voltages. Nevertheless, after experienced thermal cycling at 600 °C, the breakdown voltage of Al_2O_3 coating without buffer layer drops abruptly, while that of Al_2O_3 coatings with buffer layer decreases slightly.

Excellent resistivity (10^{15} Ω cm) and high breakdown voltage (110 kV/mm) have been achieved for the deposited $\text{Ni}/\text{Al}_2\text{O}_3$ or $\text{NiAl}/\text{Al}_2\text{O}_3$ coating. The electrical insulating properties dropped to a certain extent after thermal cycling at 600 °C up to complete failure after eight cycling tests probably due to the residual mismatch of the thermal expansion coefficient between Cu and Al_2O_3 . The amorphous structure may also be an additional cause of insulating properties

degradation after thermal cycling at 600 °C. It has been reported that amorphous coating presented worse insulating properties if compared to crystalline coating [15].

4. Conclusions

Al_2O_3 coatings with a Ni-based buffer layer on a Cu substrate were deposited by the EBE technique. The Al_2O_3 coatings did not contain impurities from the buffer layer or the substrate, and were amorphous, of good stoichiometry, and with no cracks or trace of column structure. The Ni-based buffer layer played a key role on improving the adhesion of the Al_2O_3 coating to the Cu substrate, and in suppressing the diffusion of Cu from the substrate into the Al_2O_3 coating at high temperature. Excellent resistivity (10^{15} Ω cm) and high breakdown voltage (110 kV/mm) have been achieved for the deposited $\text{Al}_2\text{O}_3/\text{Ni}$ -based buffer layer system.

References

- [1] Y. Jeliyazova, R. Franchy, Appl. Surf. Sci. 187 (2002) 51.
- [2] M. Voigt, M. Sokolowski, Mater. Sci. Eng. B 109 (2004) 99.
- [3] M. Yoshitake, B. Mebarki, T.T. Lay, Surf. Sci. 511 (2002) L313.
- [4] N. Bahlawane, Thin Solid Films 396 (2001) 126.
- [5] W. Zhang, W. Liu, C. Wang, Ceram. Int. 29 (2003) 427.
- [6] J.C. Nable, S.L. Suib, F.S. Galasso, Surf. Coat. Technol. 186 (2004) 423.
- [7] S.K. Pradhan, P.J. Reucroft, Y. Ko, Surf. Coat. Technol. 176 (2004) 382.
- [8] O. Zywitzki, K. Goedicke, H. Morgner, Surf. Coat. Technol. 151–152 (2002) 14.
- [9] M. Voigt, M. Sokolowski, Mater. Sci. Eng. B 109 (2004) 99.
- [10] K.S. Shamala, L.C.S. Murthy, K. Narasimha Rao, Mater. Sci. Eng. B 106 (2004) 269.
- [11] D.-H. Kuo, K.-H. Tzeng, Thin Solid Films 460 (2004) 327.
- [12] H. Bartzsch, D. Gloß, B. Bocher, P. Frach, K. Goedicke, Surf. Coat. Technol. 174–175 (2003) 774–778.
- [13] M.D. Groner, J.W. Elam, F.H. Fbreguette, S.M. George, Thin Solid Films 413 (2002) 186–197.
- [14] R. Li, Ceramics and Metal Composite Material, Metallurgy Industry Press, PR China, 2002.
- [15] A. Ide-Ektessabi, H. Uehara, S. Kamitani, Thin Solid Films 447–448 (2004) 388.